PROCEEDINGS OF SPIE

SPIEDigitalLibrary.org/conference-proceedings-of-spie

Micro-Raman spectroscopic characterization of ZnO quantum dots, nanocrystals, and nanowires

Irene Calizo, Khan A. Alim, Vladimir A. Fonoberov, Sivashankar Krishnakumar, Manu Shamsa, et al.

Irene Calizo, Khan A. Alim, Vladimir A. Fonoberov, Sivashankar Krishnakumar, Manu Shamsa, Alexander A. Balandin, Russell Kurtz, "Micro-Raman spectroscopic characterization of ZnO quantum dots, nanocrystals, and nanowires," Proc. SPIE 6481, Quantum Dots, Particles, and Nanoclusters IV, 64810N (6 February 2007); doi: 10.1117/12.713648

SPIE.

Event: Integrated Optoelectronic Devices 2007, 2007, San Jose, California, United States

Downloaded From: https://www.spiedigitallibrary.org/conference-proceedings-of-spie on 4/14/2018 Terms of Use: https://www.spiedigitallibrary.org/terms-of-use

Micro-Raman spectroscopic characterization of ZnO quantum dots, nanocrystals and nanowires

Irene Calizo[a], Khan A. Alim[b], Vladimir A. Fonoberov[a], Sivashankar Krishnakumar[a], Manu Shamsa[a], Alexander A. Balandin[*a] and Russell Kurtz[b]
[a] Nano-Device Laboratory, Department of Electrical Engineering, University of California – Riverside, Riverside, California 92521 USA
[b] Applied Technologies Division, Physical Optics Corporation, 20600 Gramercy Place, Building #100, Torrance, CA 90501 USA

ABSTRACT

Nanostructures, such as quantum dots, nanocrystals and nanowires, made of wurtzite ZnO have recently attracted attention due to their proposed applications in optoelectronic devices. Raman spectroscopy has been widely used to study the optical phonon spectrum modification in ZnO nanostructures as compared to bulk crystals. Understanding the phonon spectrum change in wurtzite nanostructures is important because the optical phonons affect the light emission and absorption. The interpretation of the phonon peaks in the Raman spectrum from ZnO nanostructures continues to be the subject of debates. Here we present a comparative study of micro-Raman spectra from ZnO quantum dots, nanocrystals and nanowires. Several possible mechanisms for the peak position shifts, i.e., optical phonon confinement, phonon localization on defects and laser-induced heating, are discussed in details. We show that the shifts of ~2 cm^{-1} in non-Resonant spectra are likely due to the optical phonon confinement in ZnO quantum dots with the average diameter of 4 nm. The small shifts in the non-Resonant spectra from ZnO nanowires with the diameter ~20 nm – 50 nm can be attributed to either defects or large size dispersion, which results in a substantial contribution from nanowires with smaller diameters. The large red-shifts of ~10 cm^{-1} in the resonant Raman spectrum from nanocrystals were proved to be due to local laser heating.

Keywords: micro-Raman spectroscopy, ZnO nanostructures, phonon confinement, laser heating, wurtzite quantum dots

1. INTRODUCTION

Nanostructures made of zinc oxide (ZnO), a wide-bandgap semiconductor, have recently attracted a lot of attention due to their proposed applications in low-voltage and short-wavelength (368 nm) electro-optical devices, transparent ultraviolet (UV) protection films, gas sensors, and varistors [1-10]. It is expected that in ZnO nanostructures one may eliminate some unwanted properties of bulk ZnO, such as weak exciton emission in comparison with the defect related (deep-level) visible emission, while keeping or enhancing the desirable properties such as large exciton binding energy (~60 meV). The large exciton binding energy and strong exciton emission would allow for stable high-yield luminescence from ZnO nanostructures even at room temperature.

Raman spectroscopy presents a powerful tool for identifying specific materials in complex structures and for extracting useful information on properties of nanoscale objects. At the same time the origin of Raman peak deviation from the bulk values is not always well understood for new material systems. There are three main mechanisms that can induce phonon shifts in the free-standing undoped ZnO nanostructures: (i) phonon confinement by the quantum dot boundaries; (ii) phonon localization on defects (oxygen deficiency, zinc excess, surface impurities, etc.); and (iii) the laser-induced heating in nanostructure ensembles.

In this paper we report results of the non-resonant and resonant Raman scattering studies of an ensemble of ZnO quantum dots with the average diameter of 4 nm, ZnO nanocrystals with the average diameter of 20 nm and ZnO

* balandin@ee.ucr.edu; phone 951 827-2351; fax 951 827-2425; ndl.ee.ucr.edu

Quantum Dots, Particles, and Nanoclusters IV, edited by Kurt G. Eyink, Diana L. Huffaker, Frank Szmulowicz,
Proc. of SPIE Vol. 6481, 64810N, (2007) · 0277-786X/07/$18 · doi: 10.1117/12.713648

Downloaded From: https://www.spiedigitallibrary.org/conference-proceedings-of-spie on 4/14/2018 Terms of Use: https://www.spiedigitallibrary.org/terms-of-use

nanowires with the diameter in the range from 20 nm to 50 nm (see Figure 1). The quantum dot and nanocrystal samples were prepared by the wet chemistry means while the nanowire samples were grown using the vapor phase transport method. The distinction between the two specific types of nanostructures – quantum dots and nanocrystals – is related to their size in comparison with the exciton diameter in ZnO. The average quantum dot diameter is 4 nm, which is of the order of the exciton diameter in ZnO (~ 2 nm), while the average diameter of ZnO nanocrystal studied in this work is 20 nm, which is much larger than the exciton diameter. This means that if the quantum dots were close to ideal (without defects) the charge carriers were in the regime of intermediate quantum confinement [1]. Although the charge carriers do not experience quantum confinement effects in ZnO nanocrystals, their recombination properties are expected to be different from those of bulk ZnO due to the larger surface-to-volume ratio in nanocrystals. Since quantum dots have even larger surface-to-volume ratio, the presence of many surface defects may affect the emission and absorption properties of ZnO quantum dots stronger than the quantum confinement. Thus, the distinction between quantum dots and nanocrystals is important for the proposed optoelectronic applications of ZnO nanostructures. In this paper we examine how the size differences affect the Raman scattering spectra from wurtzite ZnO nanostructures.

Based on the obtained experimental data, we have been able to identify the origin of the observed phonon frequency shifts in each of the nanostructure samples. It has been found that the optical phonon confinement results in phonon frequency shifts of only few cm^{-1}. At the same time, the ultraviolet laser heating of the ensemble was found to induce a large red shift of the phonon frequencies. The obtained experimental results are in excellent agreement with the theory of the optical phonons in wurtzite nanocrystals developed by Fonoberov and Balandin [11-13]. The theory predicts that the asymmetry of the wurtzite crystal lattice leads to the quantum dot shape-dependent splitting of the frequencies of polar optical phonons in a series of discrete frequencies. The obtained experimental and theoretical results allow one to unambiguously identify phonon peaks in the Raman spectrum of ZnO nanostructures. The results shed new light on the optical phonons in ZnO nanostructures and can be used for their optimization for the optoelectronic applications.

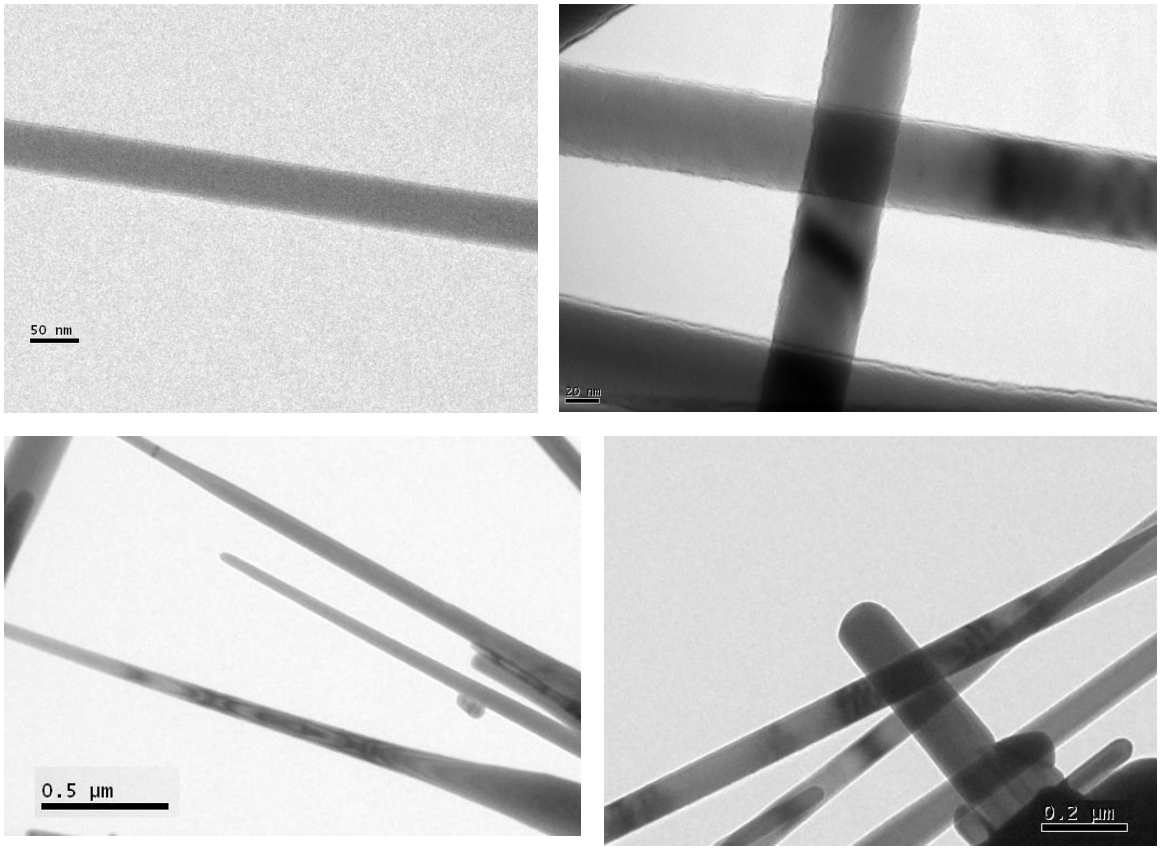

Figure 1: High-resolution transmission electron microscope (TEM) images of the ZnO nanowires studied in this work. The micrographs have been obtained with FEI-PHILIPS CM 300 instrument.

Downloaded From: https://www.spiedigitallibrary.org/conference-proceedings-of-spie on 4/14/2018 Terms of Use: https://www.spiedigitallibrary.org/terms-of-use

2. EXPERIMENTAL PROCEDURE

As a reference bulk crystal, we have used ZnO wafer (University wafer) with the dimensions 5 × 5 × 0.5 mm^3. The *c*-axis of wurtzite ZnO was parallel to the sample face and at 45° to the sample edges. The sample face coincided with the a-plane (11-20) of wurtzite ZnO. The quantum dots and nanocrystals, which were produced by wet chemistry, had nearly spherical shape and the average diameter 20 nm and 4 nm, respectively. The nanocrystals form a loose powder of white color while quantum dots were dissolved in water. The nanocrystal sample was 99.5% pure and contained impurities of Cu, Mn and Pd, which is typical of the ZnO nanostructures produced by wet chemistry. A high-resolution transmission electron microscope (TEM) FEI-PHILIPS CM 300 was used to investigate the size and shape of ZnO quantum dots, nanocrystals and nanowires. Figure 1 shows TEM images of the examined nanowire samples while Figure 2 presents the quantum dot and nanocrystal samples. The TEM data presented in Figure 1 indicate that there are regions, where the nanowire diameter is constant along the length of the nanowire and there is substantial separation among single nanowires. At the same time, there are regions where the nanowire diameter changes from 50 nm to a very small one and the nanowires are densely packed. Although micro-Raman spectroscopy allows for some spatial resolution by focusing the excitation laser into different micrometer-size spots, we expect that the signal contains response from nanowires of variable diameters. The ZnO nanowires (provided by NanoLab, Inc.) shown in Figure 1 were synthesized with a vapor phase transport process in a two zone tube furnace via catalyzed crystal growth. The Zn source was Zn nitrate hexahydrate deposited onto graphite powder.

A Renishaw micro-Raman spectrometer RM 2000 with the visible (488 nm and 633 nm) and UV (325 nm) excitation lasers was employed to measure the non-resonant and resonant Raman spectra of ZnO samples. The number of gratings in the Raman spectrometer was 1800 for the visible laser. All spectra were taken in the backscattering configuration at room temperature. To avoid the saturation of CCD spectrometer, we used a low 1.5 mW laser power while measuring Raman spectra for 4-nm diameter nanocrystals.

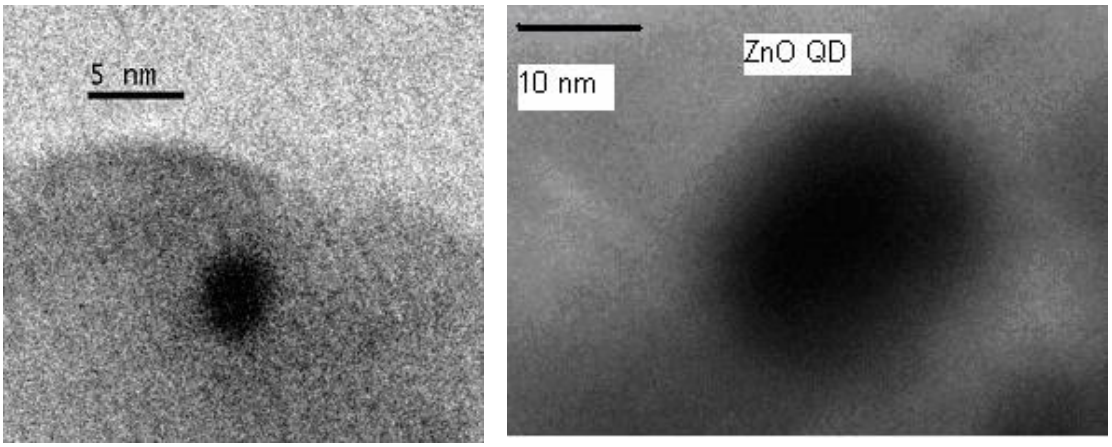

Figure 2: High-resolution transmission electron microscope (TEM) images of the ZnO quantum dots (left panel) and ZnO nanocrystals (right panel) studied in this work. The average diameter of the quantum dot is ~ 4 nm while the average diameter of the nanocrystals is ~20 nm. The micrographs have been obtained with FEI-PHILIPS CM 300 instrument.

3. EXPERIMENTAL RESULTS

Wurtzite structure belongs to the space group C_{6v}^4 with two formulae units per primitive cell, where all atoms occupy C_{3v} sites. The Raman active zone-center optical phonons predicted by the group theory are $A_1+2E_2+E_1$. The phonons of A_1 and E_1 symmetry are polar phonons and, hence, exhibit different frequencies for the transverse optical (TO) and

Downloaded From: https://www.spiedigitallibrary.org/conference-proceedings-of-spie on 4/14/2018 Terms of Use: https://www.spiedigitallibrary.org/terms-of-use

longitudinal optical (LO) phonons. In wurtzite ZnO crystals, the non-polar phonon modes with symmetry E_2 have two frequencies, E_2 (high) is associated with oxygen atoms and E_2 (low) is associated with Zn sublattice. The described phonon modes have been reported in the Raman scattering spectra of bulk ZnO [10, 14]. In Figure 3 we present a typical non-resonant Raman scattering spectrum from ZnO nanowire obtained under the 633-nm non-resonant excitation. For comparison, the phonon peaks observed in bulk ZnO crystals are summarized in Table I.

Table I Raman active phonon mode frequencies (in cm^{-1}) for bulk ZnO

E_2(low)	A_1(TO)	E_1(TO)	E_2(high)	A_1(LO)	E_1(LO)
102	379	410	439	574	591

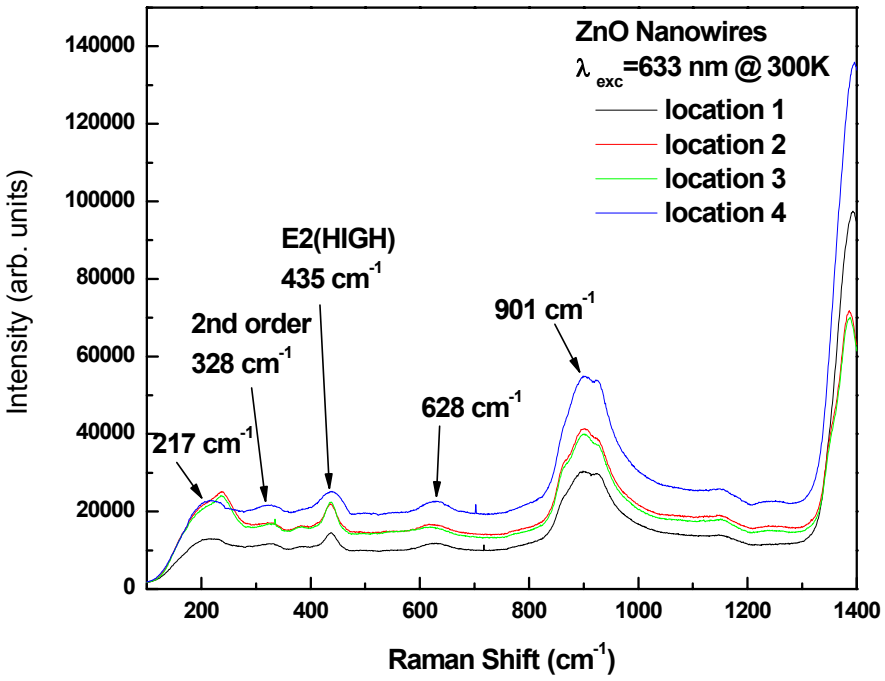

Figure 3: Non-resonant Raman spectra from ZnO nanowires under 633 nm excitation. The results are obtained in the backscattering configuration at room temperature.

Since TEM characterization (see Figure 1) revealed the non-uniformities in the sample structure and clustering, the measurements were taken from several different locations (spots) on the sample-holder covered with the ZnO nanowire material. The analysis of the data presented in Figure 3 indicates that the phonon peak position is consistent for different locations and the only difference in the peak intensity comes from the different amount of ZnO material in the interaction volume. Under the 633-nm excitation the E2 (high) peak is shifted by ~ 4 cm^{-1} from its bulk value. Some of the peaks revealed under the 633-nm excitation are the second order peaks (e.g., 901 cm^{-1}). Figure 4 shows that, under 488-nm non-resonant excitation, the E_2 (high) peak has the same position, 435 cm^{-1}, as in the previous plot. The peak at 586 cm^{-1} can be E1 (LO) peak shifted from its bulk value by ~5 cm^{-1}. Few inverse centimeters (1-2 cm^{-1}) red shifts were observed for peaks in the Raman spectra from ZnO nanocrystals (see also our data reported in Ref. [9-10]). The observed shifts for the nanowires with 20 nm – 50 nm diameter and nanocrystals with the average 20 nm diameter are unlikely due to the optical phonon confinement effect, which is expected to manifest itself for smaller structures. The spatial confinement of optical phonons was studied by Richter *et al.* [15], who showed that the Raman spectra of nanocrystalline semiconductors are red-shifted and broadened due to the relaxation of the *q*-vector selection rule in the

Downloaded From: https://www.spiedigitallibrary.org/conference-proceedings-of-spie on 4/14/2018 Terms of Use: https://www.spiedigitallibrary.org/terms-of-use

finite size nanocrystals. Due to the Heisenberg uncertainty principal, the fundamental $q \sim 0$ Raman selection rule is relaxed for a finite size domain, allowing the participation of phonons away from the Brillouin-zone center. The phonon uncertainty goes roughly as $\Delta q \sim 1/D$, where D is the diameter of a nanocrystal or quantum dot. This spatial confinement inside quantum dots of small diameter gives rise to a red shift and asymmetric broadening of the Raman peaks in nanostructures compared to bulk crystals. Figure 5 shows the Raman spectrum from ZnO quantum dots, which indicate a small shift of ~1.5 cm^{-1} in the position of E_2 (high) phonon.

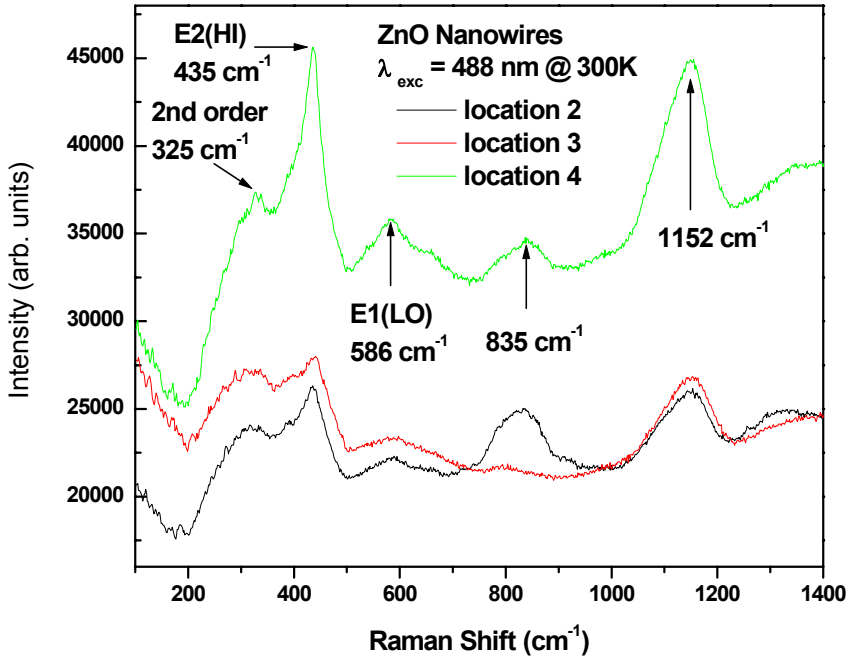

Figure 4: Non-resonant Raman spectra from ZnO nanowires under 488 nm excitation. The results are obtained in the backscattering configuration at room temperature.

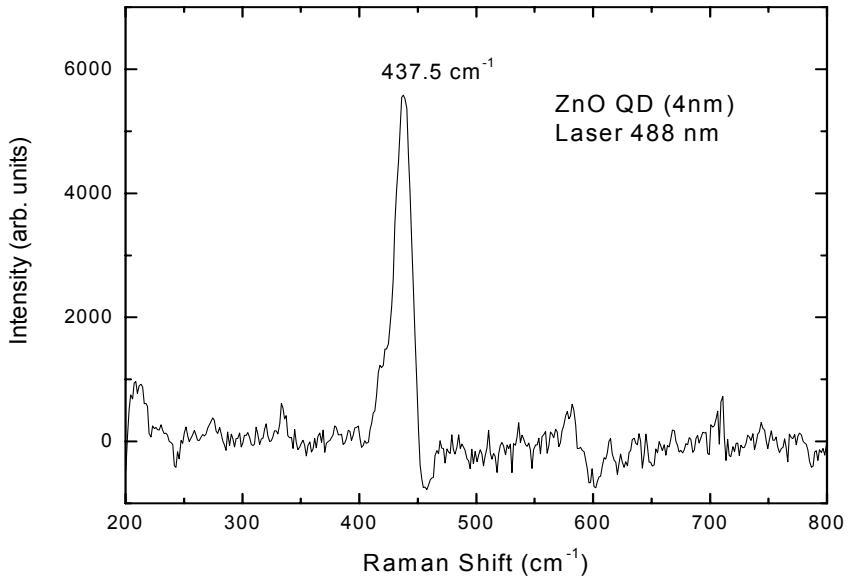

Figure 5: Non-resonant Raman spectrum from ZnO quantum dots under 488-nm excitation. The results are obtained in the backscattering configuration at room temperature.

Downloaded From: https://www.spiedigitallibrary.org/conference-proceedings-of-spie on 4/14/2018 Terms of Use: https://www.spiedigitallibrary.org/terms-of-use

In order to elucidate the possible mechanisms of the peak shifts we carried out simple calculations in the framework of the Richter [15] and Campbell [16] phenomenological models. Initially, this spatial-correlation or phonon confinement model was proposed to explain the observed shift to the lower frequency ("red shifts") and broadening of the Raman line in microcrystalline Si. In this model the Raman spectrum is given by [15-16]:

$$I(\omega) \cong \int \frac{\left|C(0,\mathbf{q})\right|^2 d\mathbf{q}}{\left[\omega - \omega(\mathbf{q})\right]^2 + \left(\Gamma_0/2\right)^2}, \tag{1}$$

where $\omega(\mathbf{q})$ is the phonon dispersion, Γ_0 is the natural line-width, $C(0,\mathbf{q})$ is the Fourier transform of the confining function and the integration is over the entire Brillouin zone. In Si the branches of the phonon dispersion decrease in the vicinity of the Γ-point. Therefore for simplicity, the integration can be approximated with the integration over a spherical Brillouin zone using the averaged dispersion curve. This model has been widely used to find the optical phonon confinement effect not only in Si, but also in Ge [17-19], TiO_2 [20] and CdS [21]. Using an approximate fitting equation for the $\omega(\mathbf{q})$ dispersion we have evaluated the expected shift in the peak positions (the value of natural line-width was assumed to be 5 cm^{-1}) [22]. Since we consider the non-polar phonons in ZnO, the extension of the model developed for Si is relatively well justified.

In Figure 6 we show the results of the calculations for ZnO quantum dots (D = 4 nm) and ZnO nanocrystals (D = 20 nm). One can see that the non-polar optical phonon, E_2 (high) can be red-shifted and strongly broadened for the small-size quantum dots while the effect is much weaker for the nanocrystals.

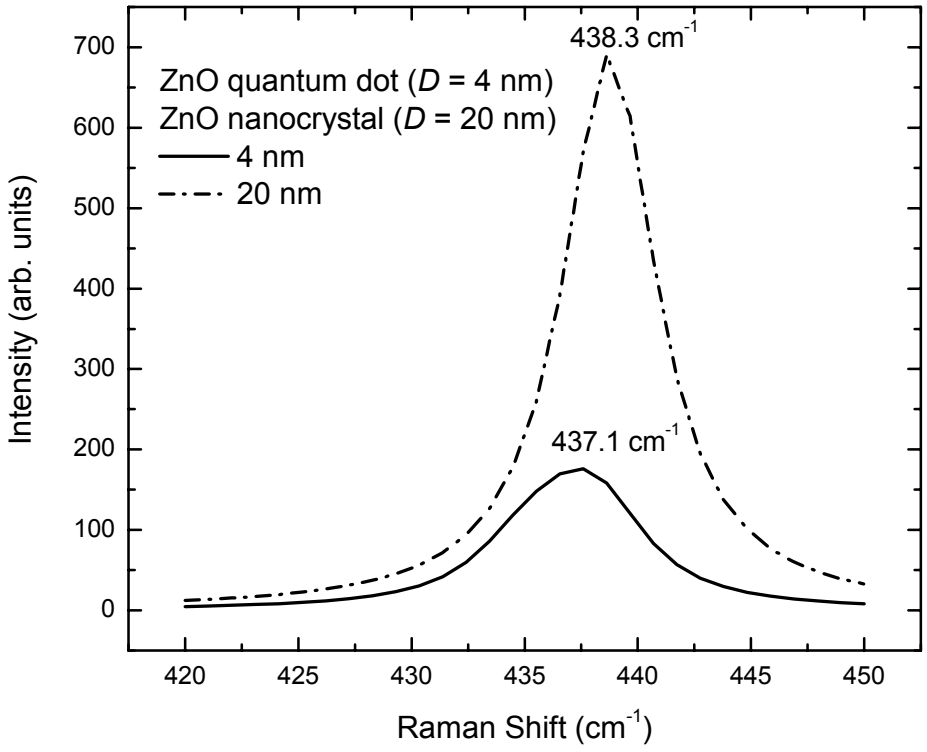

Figure 6: Simulated Raman peaks from quantum dots with the diameter 4 nm and nanocrystals with the diameter of 20 nm.

Downloaded From: https://www.spiedigitallibrary.org/conference-proceedings-of-spie on 4/14/2018 Terms of Use: https://www.spiedigitallibrary.org/terms-of-use

In Figure 7 we show the results of the calculations for the peak broadening and red shift as a function of the nanostructure diameter. The modeling results indicate that the detectable red shift due to the optical phonon confinement (for the approximated weak phonon dispersion in the center of the Brillouin zone) is expected at the diameter of about 4-5 nm. This shift is consistent with the measurements for ZnO quantum dots presented in Figure 5. At the same time it suggests that the observed ~4-5 cm^{-1} shifts in the Raman spectra from ZnO nanowires and 1-2 cm^{-1} shifts in the spectrum from ZnO nanocrystals (under non-resident excitation) cannot be attributed to the optical phonon confinement. These shifts are either due to defects in the lattice or large size dispersion, which leads to the contribution to the spectrum from smaller diameter nanostructures. Previously we reported a role of the local heating in the observed peak shifts in the spectrum from ZnO nanocrystals under resonant excitation [9-10]. At the same time the local heating effects have been ruled out for the 633 nm and 488 nm excitations.

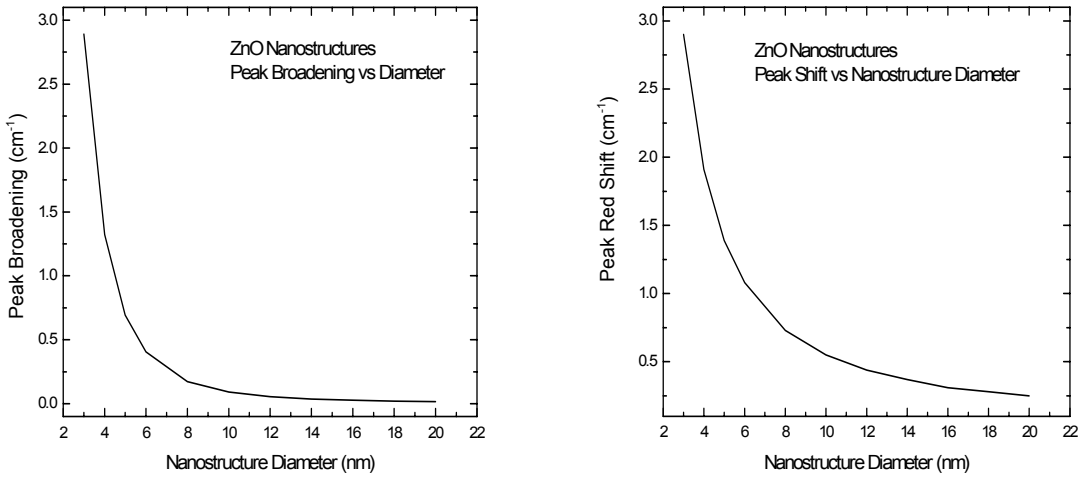

Figure 7: Simulated Raman peak broadening and its red shift from the position in bulk as the functions of the nanostructure diameter.

4. CONCLUSIONS

We reported the results of the comparative study of micro-Raman spectra from ZnO quantum dots, nanocrystals and nanowires. Several possible mechanisms for the peak position shifts, i.e., optical phonon confinement, phonon localization on defects and laser-induced heating have been discussed. Accurate interpretation of the Raman spectra from ZnO nanostructures is important for assessment of the material quality and nanostructure optimization for the proposed optoelectronic applications.

Acknowledgements

The work at UCR was supported, in part, through the DARPA – DMEA funded UCR-UCLA-UCSB Center on Nanoscience Innovation for Defense (CNID).

Downloaded From: https://www.spiedigitallibrary.org/conference-proceedings-of-spie on 4/14/2018 Terms of Use: https://www.spiedigitallibrary.org/terms-of-use

REFERENCES

1. For a review see, for example, V.A. Fonoberov and A.A. Balandin, "ZnO quantum dots: properties and optoelectronic applications," *J. Nanoelectron. Optoelectron*., **1**, 19 (2006); V.A. Fonoberov and A.A. Balandin, "Properties of GaN and ZnO quantum dots," in *Handbook of Semiconductor Nanostructures and Nanodevices*, (A.A. Balandin and K.L. Wang, Eds.), Vol. **3**, pp. 119, American Scientific Publishers, Los Angeles (2006).
2. D. W. Bahnemann, C. Kormann, and M. R. Hoffmann, "Preparation and characterization of quantum size zinc oxide: A detailed spectroscopic study," *J. Phys. Chem*. **91**, 3789 (1987).
3. E. A. Muelenkamp, "Synthesis and growth of ZnO nanoparticles", *J. Phys. Chem. B* **102**, 5566 (1998).
4. A. Wood, M. Giersig, M. Hilgendorff, A. Vilas-Campos, L. M. Liz-Marzan, and P. Mulvaney, "Size effects in ZnO: The cluster to quantum dot transition," *Aust. J. Chem*. **56**, 1051 (2003).
5. E. M. Wong and P. C. Searson, "ZnO quantum particle thin film fabricated by electrophoretic deposition," *Appl. Phys. Lett.* **74**, 2939 (1999).
6. L. Guo, S. Yang, C. Yang, P. Yu, J. Wang, W. Ge, and G. K. L. Wong, "Highly monodispersed poly-capped ZnO nanoparticles: preparation and optical properties," *Appl. Phys. Lett.* **76**, 2901 (2000).
7. H. Zhou, H. Alves, D. M. Hofmann, W. Kriegseis, B. K. Meyer, G. Kaczmarczyk, and A. Hoffmann, "Behind the weak excitonic emission of ZnO quantum dots: ZnO/$Zn(OH)_2$ core-shell structure," *Appl. Phys. Lett.* **80**, 210 (2002).
8. A. Dijken, E. A. Muelenkamp, D. Vanmaekelbergh, and A. Meijerink, "The kinetics of the radiative nonradiative processes in nanocrystalline ZnO particles upon photoexcitations," *J. Phys. Chem. B* **104**, 1715 (2000).
9. K.A. Alim, V.A. Fonoberov and A.A. Balandin, "Origin of optical phonon frequency shifts in ZnO quantum dots," *Appl. Phys. Lett.* **86**, 053103 (2005).
10. K. Alim, V.A. Fonoberov, M. Shamsa and A.A. Balandin, "Micro-Raman investigation of optical phonons in ZnO quantum dots," *J. Appl. Phys*. **97**, 124313 (2005).
11. V.A. Fonoberov and A.A. Balandin, "Polar optical phonons in wurtzite spheroidal quantum dots: theory and applications to ZnO and ZnO/MgZnO nanostructures," *J. Phys: Condens. Matter* **17**, 1085 (2005).
12. V.A. Fonoberov and A.A. Balandin, "Interface and confined optical phonons in wurtzite nanocrystals," *Phys. Rev. B* **70**, 233205 (2004).
13. V.A. Fonoberov and A.A. Balandin, "Interface and confined polar optical phonons in ZnO quantum dots," *Physica Status Solidi (c)* **11**, 2650 (2004).
14. N. Ashkenov, B. N. Mbenkum, C. Bundesmann, V. Riede, M. Lorenz, D. Spemann, E. M. Kaidashev, A. Kasic, M. Schubert, M. Grundmann, G. Wagner, H. Neumann, V. Darakchieva, H. Arwin, and B. Monemar, "Infrared dielectric functions and phonon modes of high-quality ZnO films," *J. Appl. Phys. **93***, 126 (2003).
15. H. Richter, Z. P. Wang, and L. Ley, "The one phonon Raman spectrum in microcrystalline silicon," *Solid State Commun*. **39**, 625 (1981).
16. I. H. Chambell and P. M. Fauchet, "The effects of microcrystal size and shape on the one phonon Raman spectra of crystalline semiconductors," *Solid State Commun.* **58**, 739 (1986).
17. M. Fujii, S. Hayashi and K. Yamamoto, "Growth of Ge Microcrystals in SiO_2 Thin Film Matrices: A Raman and Electron Microscopic Study," *Jpn. J. Appl. Phys*. **30**, 687 (1991).
18. Y. Sasaki and C. Horie, "Resonant Raman study of phonon states in gas-evaporated Ge small particles," *Phys. Rev. B* **47**, 3811 (1993).
19. S. Guha, M. Wall, L. L. Chase, "Growth and characterization of Ge nanocrystals," *Nucl. Instrum. Methods Phys. Res. B* **147**, 367 (1999).
20. D. Bersani, P. P. Lottici, X. Z. Ding, "Phonon confinement effects in the Raman scattering by TiO_2 nanocrystals," *Appl. Phys. Lett.* **72**, 73 (1998).
21. M. I. Vasilevskiy, A. G. Rolo, M. J. M. Gomes, "One-phonon Raman scattering from arrays of semiconductor nanocrystals," *Solid State Commun.* **104**, 381 (1997).
22. K.A. Alim, "Micro-Raman and photoluminescence investigation of ZnO and hybrid bio-inorganic nanostructures," Ph.D. dissertation, Department of Electrical Engineering, University of California – Riverside, Riverside, CA (2006).

Downloaded From: https://www.spiedigitallibrary.org/conference-proceedings-of-spie on 4/14/2018 Terms of Use: https://www.spiedigitallibrary.org/terms-of-use